MOLECULAR PHARMACOLOGY, 21:351-361

Actions of the Histrionicotoxins at the Ion Channel of the Nicotinic Acetylcholine Receptor and at the Voltage-Sensitive Ion Channels of Muscle Membranes

C. E. SPIVAK,[1] M. A. MALEQUE,[2] A. C. OLIVEIRA,[3] L. M. MASUKAWA,[4] T. TOKUYAMA,[5] J. W. DALY,[6] AND E. X. ALBUQUERQUE[2]

Department of Pharmacology and Experimental Therapeutics, University of Maryland School of Medicine, Baltimore, Maryland 21201, and Laboratory of Bioorganic Chemistry, National Institutes of Arthritis, Metabolism and Digestive Diseases, Bethesda, Maryland 20215

Received May 4, 1981; Accepted October 5,1981

SUMMARY

Various histrionicotoxins tested on frog nerve-muscle preparations showed a qualitative family resemblance to one another. They blocked the nerve-evoked muscle twitch and depressed both the peak amplitudes and the decay time constants of end-plate currents. During repetitive stimulation they progressively decreased the rate of rise and prolonged the falling phase of muscle action potentials, the latter resulting, at least in part, from blockade of voltage-sensitive potassium channels. These results indicated that the histrionicotoxins act at three membrane channels: the channel associated with the acetylcholine receptor, the sodium channel, and the potassium channel. Closer study of perhydrohistrionicotoxin suggested either two topographically distinct sites of action at the acetylcholine receptor-ion channel complex, or one site and two ion channel complex conformations. One site or conformation only alters the kinetics of channel closure. As these sites become saturated, the end-plate current decay time constant asymptotically approaches a limiting value. The other site or conformation prevents the channel from opening altogether. Further analysis indicated that the binding site for perhydrohistrionicotoxin that alters the kinetics of channel closure has an affinity constant of 0.1 μM^{-1} at −90 mV and that this affinity may be sensitive to the membrane potential. The lipid protein interface is a suggested site of histrionicotoxin action, common to the three channels studied here as well as to other intrinsic membrane proteins affected by histrionicotoxins.

INTRODUCTION

The nicotinic AChR[7] is an intrinsic membrane protein which, upon binding ACh, opens an associated aqueous pore (or channel) through which cations diffuse down their respective electrochemical potential gradients. In isolated muscles, in membrane fragments, and in purified, detergent-solubilized form, the AChR is found to be highly vulnerable to blockade by a wide variety of drugs and toxins (e.g., see ref. 1). Three distinct mechanisms for blockade by drugs may be clearly delineated: desensitization, competition for the agonist recognition site, and occlusion of the channel. Desensitization may be operationally defined as a fade in receptor response that proceeds when an agonist is applied repeatedly or for prolonged periods. The molecular correlate of desensitization is still unknown. It is not even known how many "desensitized" states there are. Competition for the agonist recognition site is the chief mechanism whereby agents such as (+)-tubocurarine seem to act. By occupying the ACh recognition site, these agents exclude ACh while leaving the channel closed. Their blockade can be

This study was supported in part by United States Public Health Service Grant NS-12063 and by United States Research Office Grant DAAG 29-78-G-0203. The computer time for this project was supported in part through the facilities of the Computer Science Center of the University of Maryland.

[1] University of Maryland School of Medicine. Present address, Addiction Research Center, National Institute on Drug Abuse, c/o University of Maryland School of Medicine.

[2] University of Maryland School of Medicine.

[3] University of Maryland School of Medicine. Recipient of a Postdoctoral Fellowship from the Fundacão de Amparo a Pesquisa do Estádo de São Paulo, Brasil. Present address, Department of Pharmacology, University of São Paulo, São Paulo, Brazil.

[4] University of Maryland School of Medicine. Present address, Department of Neurology, Stanford University Medical Center, Stanford, Calif.

[5] National Institute of Arthritis, Metabolism and Digestive Diseases. Present address, Department of Chemistry, Osaka City University, Osaka, Japan.

[6] National Institute of Arthritis, Metabolism and Digestive Diseases.

[7] The abbreviations used are: ACh, acetylcholine; AChR, the entire macromolecular complex comprising the recognition site for acetylcholine, the channel, and all of the structural subunits that form them and link them together; HTX, histrionicotoxin; epc, end-plate current; τ, decay time constant; epp, end-plate potential; mepp, miniature end-plate potential; hdt, half-decay time.

0026-895X/82/020351-11$02.00/0

reversed by raising the agonist concentration. Occlusion of the opened ion channel by drugs is a widely cited mechanism that seems to apply to certain local anesthetics and a variety of other drugs (e.g., see ref. 1). The blockade by these agents behaves kinetically as if the drug were occluding the channel, although other sites of action are equally compatible with the evidence. Other mechanisms for blocking or modifying the AChR are likely, and agents that highlight these may be of great use in elucidating otherwise obscure details of AChR function.

HTX is the parent member of a class of spiropiperodine alkaloids isolated from neotropical frogs of the family *Dendrobatidae* (2, 3). Histrionicotoxin and its perhydro derivative block neuromuscular transmission (e.g., see refs. 4–8) at a site or sites apart from the recognition site for ACh (e.g., see refs. 9–12). At the frog neuromuscular junction, histrionicotoxins depress the epc peak amplitude and shorten the decay time constant (τ) (5, 7). The depression in peak amplitude is accompanied by a time and voltage dependence seen as nonlinearity and hysteresis in the peak current-voltage relationship (5, 7, 13). Histrionicotoxin also produces use-dependent effects: epc peak amplitudes (5, 7) and depolarizing responses to iontophoretically applied ACh (4–6, 14) are depressed, and the muscle action potential falling phase is prolonged during repetitive stimulation (4–6). It was not known whether these various effects of histrionicotoxin were due to interaction at one site or at a number of sites. Binding studies of radioactive H_{12}-HTX to preparations from *Torpedo* electroplax have suggested the presence of one class of sites associated with the ACh-receptor channel complex (9, 11, 15–18). It would appear probable that another site is associated with potassium channels and is responsible for the prolongation of the muscle action potential falling phase and potentiation of directly elicited muscle twitch. Structure-activity profiles of various natural and synthetic histrionicotoxins have now been investigated in frog neuromuscular preparations. These alkaloids alter responses to ACh, the kinetics of the epc, and the action potential rate of rise and falling phase, suggesting that they interact with four or more classes of sites. These include possibly two associated with the AChR, one with the sodium channel, and one with the potassium channel. Results from detailed investigations of H_{12}-HTX suggest at least two different sites, or that two different conformations of the acetylcholine receptor-channel complex interact with histrionicotoxins. When H_{12}-HTX binds to one of these sites (or conformations), the rate constant for channel closure is enhanced, and when it binds to the other site (or conformation), the channel simply does not open. Binding to the latter site may be responsible for the use-dependent blockade by histrionicotoxins seen during tetanus.

MATERIALS AND METHODS

All data were derived from sartorius muscles, with or without the attached sciatic nerve, from the frog *Rana pipiens*. The muscles were bathed in frog Ringer's solution composed as follows (millimolar concentrations): NaCl, 115; KCl, 2.0; $CaCl_2$, 1.8; Na_2HPO_4, 1.3; and NaH_2HPO_4, 0.7. To prevent twitch during epc experiments, muscles were pretreated for 60–70 min with frog Ringer's solution to which 600 mmoles of glycerol were added per liter (19). All experiments were performed at 21–23°.

Twitch data were recorded from muscles under 2–3 g of resting tension, connected to a Grass FT 03 force displacement transducer. Muscles were stimulated directly or indirectly (via the nerve) at 0.05 Hz as described previously (6). The muscle was allowed to stabilize in the organ bath for at least 30 min before the toxin solution was added.

For intracellular recording, muscles were slightly stretched over a plano-convex lens and pinned to paraffin blocks. Glass microelectrodes contained 3 M KCl and had resistances of 2–5 Mohms. Focal placement of electrodes in surface fibers was achieved by selecting the point on the fiber at which mepp or epp rise time was minimal (for epps this was less than 1.0 msec). Further details of the epc methodology can be found elsewhere (20). To record action potentials, two microelectrodes were inserted about 100 μm apart in a surface fiber. Current was passed through one microelectrode first to hyperpolarize the cell to usually −90 mV, and then to depolarize it (30-msec pulse) beyond threshold. The action potentials, their first derivatives (from an RC circuit), and time marks were displayed on a Tektronix 565 oscilloscope and recorded on film.

Histrionicotoxins (Fig. 1) were isolated from the neotropical frog *Dendrobates histrionicus* essentially as described in ref. 3. H_{12}-HTX was prepared by catalytic reduction of histrionicotoxin and converted to *N*-methyl-H_{12}-HTZ as described previously (3). Except as noted, the H_{12}-HTX used in this study was a racemic mixture synthesized and generously donated by Dr. Y. Kishi (Harvard University). No significant difference in po-

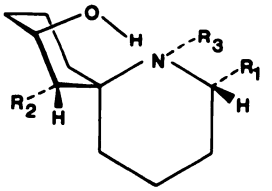

NAME	R_1	R_2	R_3
HTX	CH_2-CH=CH-C≡CH	CH=CH-C≡CH	H
ISO-H_2-HTX	CH_2-CH_2-CH=C=CH_2	CH=CH-C≡CH	H
NEO-H_2-HTX	CH_2-CH=CH-C≡CH	CH=CH-CH=CH_2	H
H_4-HTX	CH_2-CH=CH-CH=CH_2	CH=CH-CH=CH_2	H
ISO-H_4-HTX	CH_2-CH_2-CH=C=CH_2	CH=CH-CH=CH_2	H
H_6-HTX	CH_2-CH_2-CH_2-CH=CH_2	CH_2-CH_2-CH=CH_2	H
H_{12}-HTX	CH_2-CH_2-CH_2-CH_2-CH_3	CH_2-CH_2-CH_2-CH_3	H
N-METHYL-H_{12}-HTX	CH_2-CH_2-CH_2-CH_2-CH_3	CH_2-CH_2-CH_2-CH_3	CH_3
AZASPIRO-HTX	H	H	H

FIG. 1. *Structures of histrionicotoxins and of azaspiro-HTX*

tency between natural and synthetic toxins was detected in epc experiments in which equal concentrations of the toxins depressed the peak amplitudes and decay time constants to approximately equal levels. Azaspiro-HTX was synthesized by Dr. E. Gössinger (21) and provided by Dr. B. Witkop (Laboratory of Chemistry, National Institute of Arthritis, Diabetes, Digestive and Kidney Diseases, Bethesda, Md.). The structures of all of the toxins used are shown in Fig. 1. For long-term storage they were kept at −20°–25° as solids. Short-term (usually a 1-month supply) stock solutions were prepared in 95% ethanol and stored at −25°. Dilutions into frog Ringer's solution were made on the day of use.

RESULTS

Blockade of neuromuscular transmission. Except for azaspiro-HTX, all of the histrionicotoxins at 70 μM completely blocked the indirectly elicited twitch of the frog's sciatic nerve sartorius muscle preparation. The time required increased with saturation of the side chains of the histrionicotoxins (Fig. 2). The muscles were washed after 1 hr of exposure to the drug solutions, and the times to recovery were determined. HTX required about 20 min and H_{12}-HTX about 60 min until a perceptible twitch could be recorded. The H_2-, H_4-, and H_8-HTXs required times intermediate to those for HTX and H_{12}-HTX, whereas the *N*-methyl-H_{12}-HTX required about 90 min. Although these toxins act at high concentrations (>50 μM) on sodium channels to decrease the rate of rise of the muscle action potential (see below), they do not abolish the action potential at the stimulus frequencies used. We doubt, by analogy, that the toxins block neuromuscular transmission presynaptically by inhibiting the nerve action potential. In fact, HTX (at<10 μM) *increases* quantal content,[8] a phenomenon primarily attributed to the ability of the toxin to inhibit potassium channels. Potentiation of the twitch tension was seen in the presence of some of the histrionicotoxins, and is probably related to effects of these toxins on the muscle action potential (see below). Azaspiro-HTX at 100 μM blocked both the directly and indirectly elicited twitch by 90% and 50% respectively.

H_{12}-HTX blocks mepps. H_{12}-HTX depressed the spontaneous mepp amplitude in a concentration-dependent manner. For example, 1-hr treatment with 0.1, 1, 5, and 10 μM H_{12}-HTX depressed mepp amplitude to 95% (±17), 82% (±24), 65% (±11), and 52% (±12) (mean ± standard error), respectively, of pretreatment levels. At 30 μM H_{12}-HTX, the mepps in most fibers were completely blocked. Mepp frequency, around 1 Hz, was unaffected by all concentrations of H_{12}-HTX of 30 μM or less.

Effects of H_{12}-HTX on epc. H_{12}-HTX depressed both epc peak amplitudes and τs, but the approach to equilibrium seemed slow. To quantitate this temporal dependence and to establish an equilibrium time, epc peak amplitudes and τs were recorded as functions of time after adding H_{12}-HTX at varying concentrations. The results, shown in Fig. 3A, confirm the slow approach to equilibrium peak current. After 30 min the peak amplitudes decreased much less rapidly, although they still decreased even after 60 min. This continual decrease in amplitude is underestimated at high H_{12}-HTX concentrations (>10 μM) because end plates that were completely blocked, or epcs too small to record, were not averaged with the recorded ones. The epc τ, in contrast, stabilized within approximately 10 min of exposure to

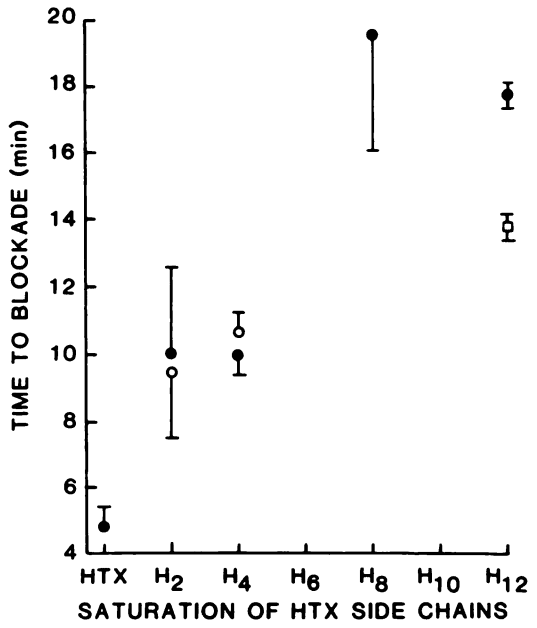

FIG. 2. *Time required to block completely the indirectly elicited twitch of frog sartorius muscles as a function of saturation of histrionicotoxin side chains*

○, "Iso" compounds; ● at H_2, neo-H_2-HTX; □ at H_{12}, *N*-methyl-H_{12}-HTX. Each point represents the mean ± standard error of three to six muscles.

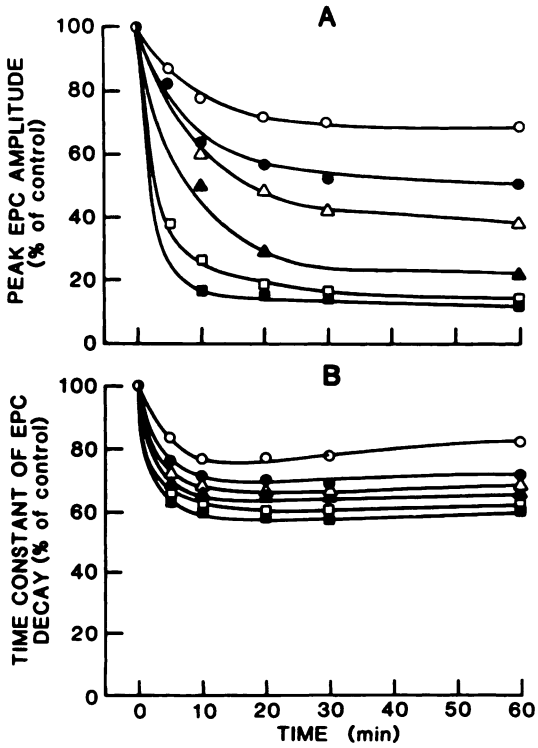

FIG. 3. *Epc peak amplitudes (A) and decay time constants (B) shown as functions of time after treating a muscle with various concentrations of H_{12}-HTX*

The concentrations of H_{12}-HTX used were 2 (○), 5 (●), 10 (△), 20 (▲), 30 (□), and 40 (■) μM. Each symbol represents the mean of 12–15 fibers from 3–5 muscles.

[8] E. X. Albuquerque, unpublished observations.

the toxin (Fig. 3B). These two markedly different times to equilibrium provide evidence for two different sites (or conformations) responsible for the toxin's two effects on the epc. Because of the slow approach to equilibrium for peak amplitude, all subsequent epc studies were begun at least 30 min after adding the toxin solution to the bath.

The epc peak amplitudes and τ values are shown plotted in Fig. 4 as functions of membrane potential and H_{12}-HTX concentration. The amplitudes are progressively depressed and show some upward concavity in the third quadrant. A slow voltage and time dependence leading to hysteresis (5, 7, 8, 13) was seen but is not shown here. Because of the time dependence, which drives peak amplitudes lower at negative potentials and higher at positive ones, peak amplitudes per se at a given membrane potential are unreliable unless fast voltage jumps are used (13). Instead, slope conductance at the null potential was plotted in Fig. 4A, *inset*, as a function of H_{12}-HTX concentration. The slope conductance appears to approach saturation above 20 μM H_{12}-HTX, but we believe this to be an artificial consequence of discarding epcs too small to record.

The τ values appeared to saturate with H_{12}-HTX concentration. This is shown clearly in Fig. 4B, *inset*, where τ^{-1} is plotted against H_{12}-HTX concentration. This plot, reminiscent of a simple, saturating, ligand binding curve, is analyzed further under Discussion.

Like HTX (4–7, 14), H_{12}-HTX produced a use-dependent depression or rundown of the end-plate current amplitude when the nerve was stimulated at 25 Hz. More reproducible results were obtained at higher stimulus frequencies. In the presence of 20 μM H_{12}-HTX or 2 μM (+)-tubocurarine, trains of epcs were elicited (−90 mV) at 50 or 100 Hz followed immediately by trains at 1 Hz to measure the rate of recovery. H_{12}-HTX first enhanced facilitation (Fig. 5), a manifestation of increased ACh release from the presynaptic nerve terminal. This facilitation probably resulted when the toxin prolonged the nerve-terminal action potentials by blocking potassium channels (see below). Following this facilitation, the envelope of epcs decreased as a single exponential function of time (Fig. 5), $A = A_0 \exp(Rt) + A_\infty$, where t is time. The parameters A_∞, R, and A_0, estimated by nonlinear regression analysis (22) of all epc amplitudes from the largest to the end of the train, are given in Table 1. Both H_{12}-HTX and (+)-tubocurarine depressed the peak amplitude, but the steady-state block produced by H_{12}-HTX was more profound (89–95%) than that produced by (+)-tubocurarine (64%). The rate constants for this depression by the two drugs were similar (Table 1; the maximal peak amplitudes, however, differed by approxi-

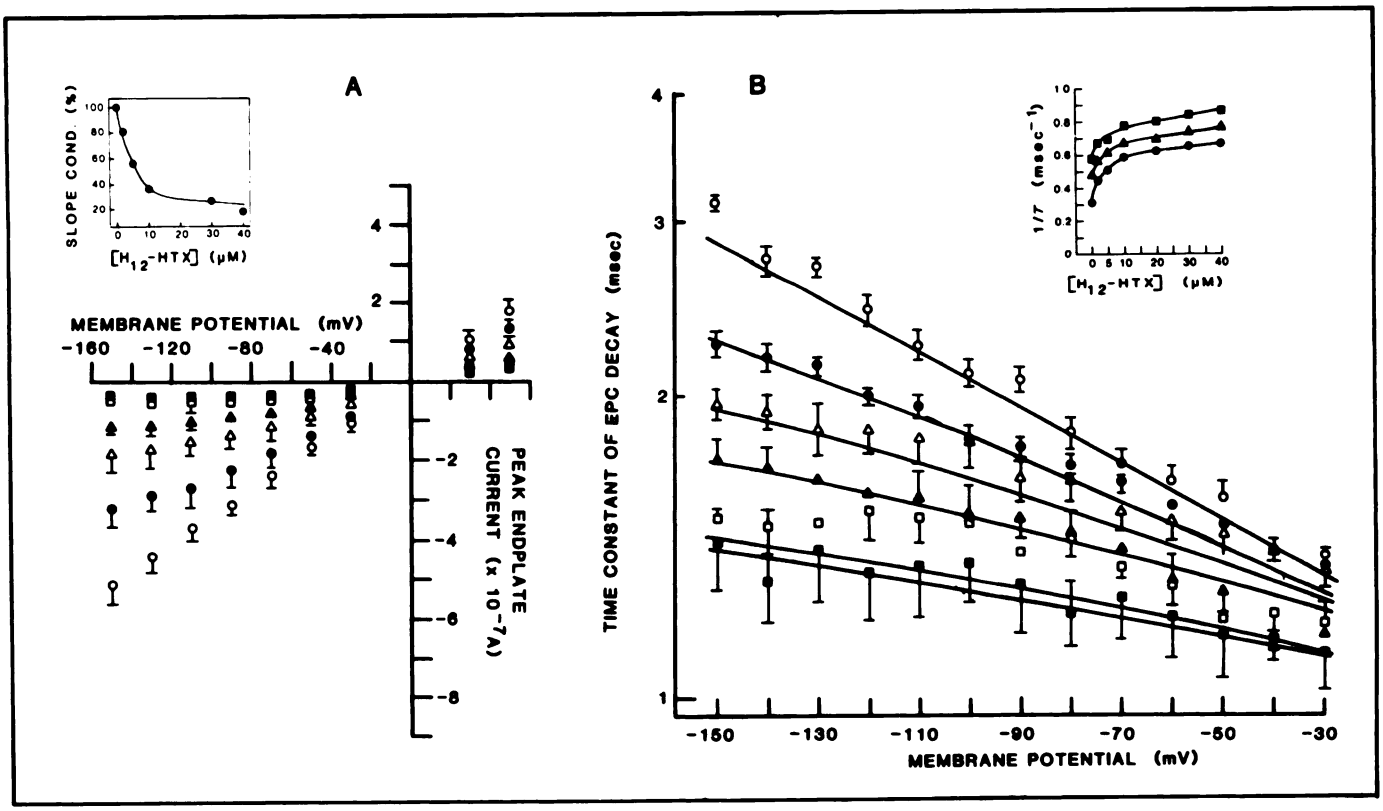

FIG. 4. *Epc peak amplitudes (A) and decay time constants (B) as a function of membrane potential under control conditions (○) and in the presence of various concentrations of H_{12}-HTX*

Each symbol represents the mean ± standard error of at least nine fibers from at least three muscles. The H_{12}-HTX concentrations used were 2 (●), 5 (△), 10 (▲), 30 (□), and 40 (■) μM. The *inset* of A shows the relative (to control) slope conductance (at 0 mV) as a function of membrane potential. The apparent approach toward an asymptote at around 20% is an artificial consequence of neglecting end plates that were completely blocked. The curves shown in B were calculated from Eq. 3 and the parameter values shown in Table 3. The *inset* of B shows reciprocal epc decay time constants at three membrane potentials plotted as functions of H_{12}-HTX concentration. Each point represents the mean of at least nine fibers from at least three muscles. Membrane potentials were −50 mV (■), −90 mV (▲), and −150 mV (●). The hyperbolic shapes suggest that $1/\tau$ approaches an asymptote as the toxin binding sites approach saturation.

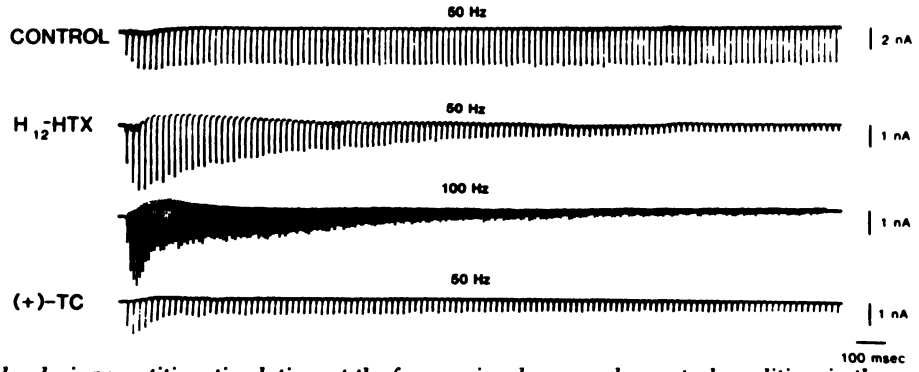

FIG. 5. *Epc amplitudes during repetitive stimulation, at the frequencies shown, under control condition, in the presence of H_{12}-HTX or in the presence of (+)-tubocurarine*

H_{12}-HTX first enhanced facilitation, probably by prolonging the action potential decay phase in the presynaptic nerve terminal. The relative depression of peak amplitude at the end of the train was more profound in the presence of H_{12}-HTX than under the other conditions shown (see Table 1). The H_{12}-HTX concentration was 20 μM, and the (+)-tubocurarine concentration was 2 μM. The membrane potential was −90 mV.

mately 3-fold). Doubling the stimulation rate doubled the rate constant for the rundown in the presence of H_{12}-HTX, a finding consistent with a cyclic model for desensitization (23). However, contrary to this model was the observation that the trains that produced the most profound steady-state block (>99%) usually had the lowest rate constants (data not shown). The recovery rate constants (five records, three cells) found in the presence of H_{12}-HTX had a median of -0.40 sec^{-1} and a range of -0.01 to -0.76 sec^{-1}. No relationship between recovery rate constant and tetanus frequency was evident. Note that, despite the rundown in epc peak amplitudes, the hdt (Table 2) remained constant. Although (+)-tubocurarine apparently depresses trains of epc amplitudes by a presynaptic mechanism (24), H_{12}-HTX, like HTX, almost certainly acts postsynaptically (7).

Effects of other histrionicotoxins and azaspiro-HTX on epc. Similar to H_{12}-HTX and in agreement with previous findings from this laboratory, HTX depressed the peak epc and introduced upward concavity in the third quadrant (Fig. 6A). The hdt was depressed (Fig. 6B), and the plot of $(\text{hdt})^{-1}$ (at −90 mV) versus HTX concentration (Fig. 6B, *inset*) seems, as in the corresponding plot for H_{12}-HTX (Fig. 4B, *inset*) to be approaching an asymptote (see Discussion).

Two other natural alkaloids, iso-H_4-HTX and H_8-HTX, were tested for effects on epcs. The current-voltage plots shown in Fig. 7 show depression, and an upward concavity in the third quadrant similar to that found with H_{12}-HTX and HTX. The slope conductance (at the null potential) in the presence of 25 μM H_8-HTX was 43% of control. To achieve the same reduction, the H_{12}-HTX concentration must be around 7 μM (see Fig. 4A, *inset*) and the HTX concentration must be around 8 μM (Fig. 6A, *inset*). A greater reduction (to 30% of control) in slope conductance was achieved by a smaller concentration (4 μM) of iso-H_4-HTX, so that one can rank these histrionicotoxins in order of potency: iso-H_4-HTX > HTX ≈ H_{12}-HTX > H_8-HTX. As shown in Fig. 7B and D, the derivatives iso-H_4-HTX and H_8-HTX depressed the epc τ, and H_8-HTX decreased the voltage sensitivity of τ. It seems likely that at higher concentrations iso-H_4-HTX would also decrease the voltage sensitivity of τ, since all of these toxins appear qualitatively similar.

Azaspiro-HTX was by far the weakest of the compounds tested in depressing epc peak amplitude. From the current-voltage plots (Fig. 8A) one estimates that a concentration of approximately 600 μM is required to reduce the slope conductance to 30% of control, indicating that this compound is only about 0.007 as potent as iso-H_4-HTX. The current-voltage plot showed some upward concavity in the third quadrant when the azaspiro-HTX concentration was 400 or 600 μM. Azaspiro-HTX did not shorten τ but rather, unlike all of the natural toxins, seemed to increase it (Fig. 8B). However, the solvent for the stock solution of azaspiro-HTX was ethanol. Ethanol at high concentrations has been shown to increase the τ of toad mepc decays (25). It is thus possible that the prolongation of τ is due to ethanol or is a summation of ethanol and azaspiro-HTX effects. The depression of peak amplitude was due to azaspiro-HTX, since ethanol increases mepc amplitude slightly (25).

Effects of histrionicotoxins on muscle action potentials. Previous studies have shown that HTX and H_{12}-HTX can prolong the half-decay time of muscle action potential and can slightly decrease its rate of rise in both

TABLE 1

Parameter estimates for epc peak amplitude during tetanic stimulation

Drug concentrations were 20 μM (H_{12}-HTX) and 2 μM [(+)-tubocurarine (TC)]. The envelope of peak amplitudes (A)was fitted by nonlinear regression analysis to the equation $A = A_0 \exp(Rt) + A_\infty$. Means ± standard deviation of parameter estimates are shown.

Drug	Stimulus frequency	No. of cells	A_0	R	A_∞	$\frac{A_\infty}{A_0 + A_\infty}$
	Hz		*namp*	*sec*$^{-1}$	*namp*	
H_{12}-HTX	50	6	17.9 ± 2.1	−1.2 ± 0.23	1.1 ± 0.69	0.058 ± 0.030
H_{12}-HTX	100	5	25.8 ± 2.3	−2.6 ± 0.13	3.12 ± 0.39	0.11 ± 0.010
(+)-TC	50	4	5.2 ± 1.2	−2.0 ± 0.36	2.9 ± 0.66	0.36 ± 0.034

TABLE 2

Decay time constants of epc during tetanic stimulation

Stimulation frequency was 50 Hz, membrane potential was −90 mV, and H_{12}-HTX concentration was 30 μM. Means ± standard error are shown.

Condition	No. of cells	τ		
		First	Fifth	Last
Control	7	1.41 ± 0.09	1.41 ± 0.08	1.33 ± 0.07
H_{12}-HTX	5	0.93 ± 0.07	1.00 ± 0.06	1.00 ± 0.02

frog and mouse muscles (4–6). These effects were more pronounced during repetitive (1-Hz) stimulation. Similar effects occurred with the other histrionicotoxins. Action potentials, directly elicited in glycerol-shocked surface fibers, in the presence of 3.5 μM toxin showed no significant deviation from control action potentials. However, during repetitive stimulation (1 Hz), marked and progressive increases in the hdt appeared (Fig. 9), suggesting effects on potassium channels. This effect was exaggerated, and a decrease in the rate of rise appeared when the toxins were present at a concentration of 70 μM (Figs. 10 and 11). The decrease in rate of rise shows that these toxins alter sodium channels. Threshold was unaffected by all toxins at concentrations up to 70 μM. Blockade of potassium channels, suggested by the prolonged decay of the action potentials, was confirmed by studies of delayed rectification. Muscles were treated with both tetrodotoxin (3 μM) to block sodium currents and an HTX solution for 30 min before current-voltage measurements (e.g., Fig. 12) of electrotonic potentials were made. All of the HTXs at 70 μM concentration partially decreased the delayed rectification, as exemplified by iso-H_2-HTX (Fig. 12).

DISCUSSION

Like HTX and H_{12}-HTX, which had been tested previously, the other four naturally occurring HTXs (Fig. 1) as well as racemic H_{12}-HTX and *N*-methyl-H_{12}-HTX blocked neuromuscular transmission (Fig. 2). A postsynaptic mechanism was implicated by the characteristic alterations of epcs. Peak amplitudes were depressed and became nonlinear functions of membrane potential, and the epc decay τ values were also depressed and showed decreased sensitivity to membrane potential. Initial binding studies disclosed that HTX, H_{12}-HTX, H_8-HTX, iso-H_4-HTX, and to a much less extent azaspiro-HTX selectively reacted with the sites located on the AChR complex but were unable to hinder binding of ACh and α-bungarotoxin at the ACh recognition sites (10). In addition, all of the toxins (at 70 μM) slowed the rate of rise and prolonged the falling phase of muscle action potentials during repetitive stimulation at 1 Hz. The decreased rate of rise reflects alterations of sodium channels, whereas the prolonged falling phase of the action potential was shown to be due, at least in part, to a blockade of potassium channels, manifested in delayed rectification experiments (Fig. 12).

The histrionicotoxins thus appear to interact with at least three separate intrinsic membrane proteins: the

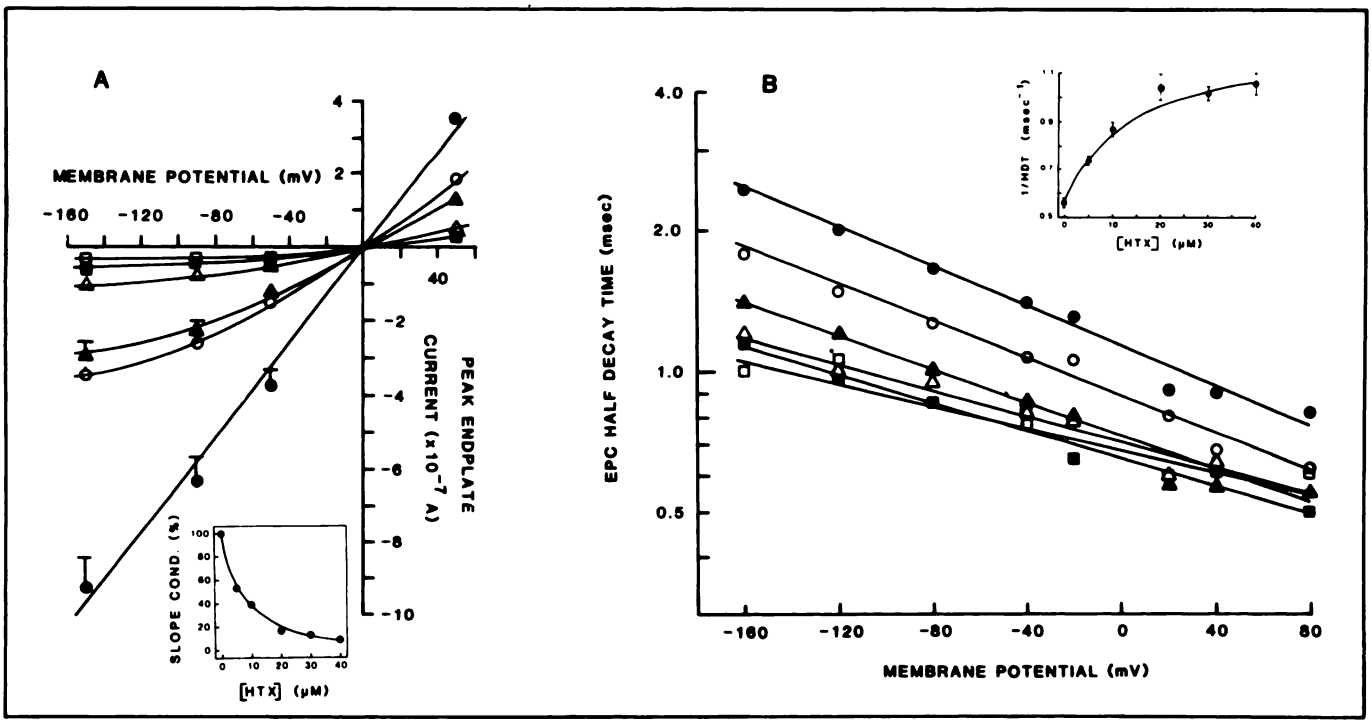

FIG. 6. *Epc peak amplitudes (A) and half-decay times (B) plotted as functions of membrane potential under control conditions (●) and in the presence of various HTX concentrations*

Each symbol represents the mean from at least nine fibers. The standard errors are shown in A except where they are smaller than the symbol. The HTX concentrations used were 5 (○), 10 (▲), 20 (△), 30 (■), and 40 (□) μM. The *inset* in A shows the slope conductance, relative to control, at 0 mV. As in the *inset* in Fig. 4A, the slope conductances are biased toward higher values at high HTX concentrations (probably >20 μM). The curves shown have no theoretical significance. The *inset* in B shows reciprocal epc half-decay times plotted as a function of HTX concentration at −90 mV membrane potential. Each symbol represents the mean ± standard error from at least nine fibers. The curve was drawn using Eq. 3 and the parameter values given in the text.

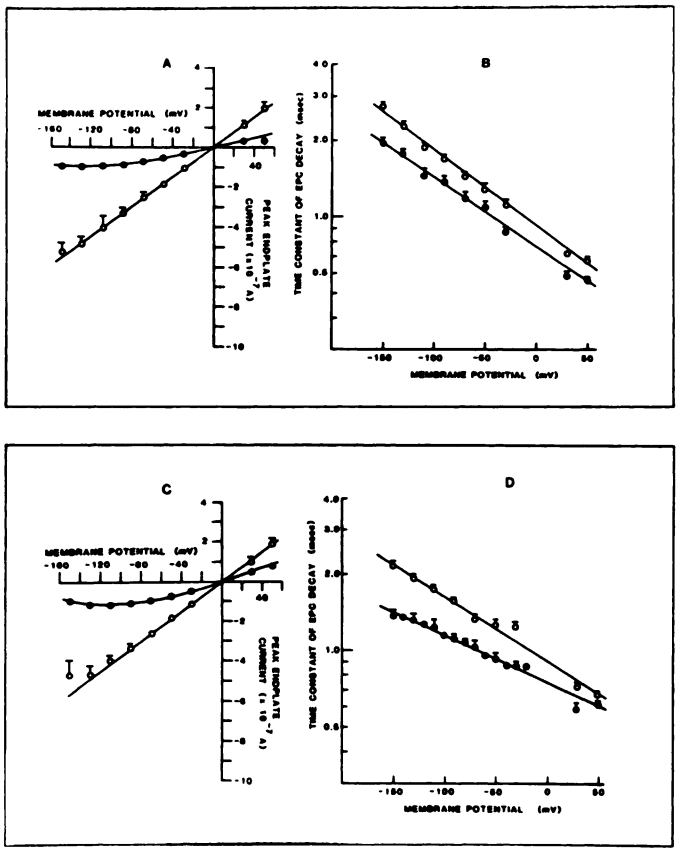

FIG. 7. *Semilogarithmic plot of tritium back-exchange kinetics*

The rate constants (k) are for the straight lines which fit the exponential appearance of ^3H in water: $1 - f = \exp(-kt)$, where f is the fraction of the ^3H which has back-exchanged into water at time t.

The toxins equilibrated with the muscles at least 30 min before recording was begun. Note that, whereas iso-H_4-HTX depressed peak amplitude slightly more than did H_8-HTX at these concentrations, H_8-HTX was somewhat more potent in depressing the decay time constants. Each symbol represents the mean ± standard error of at least seven fibers from three muscles. Standard errors smaller than the symbol are not shown.

acetylcholine receptor-ionic channel complex (AChR), the sodium channel, and the potassium channel. However, the sensitivities of these three entities to the various structural modifications vary. At the AChR, depression of the epc slope conductance followed the rank order iso-H_4-HTX > HTX ≈ H_{12}-HTX > H_8-HTX ≫ azaspiro-HTX. At the sodium channel, sensitivity, expressed as reduction in maximal rate of rise in action potentials during repetitive stimulation (70 μM toxin), followed the rank order iso-H_4-HTX > H_4-HTX > H_{12}-HTX > iso-H_2-HTX > neo-H_2-HTX > H_8-HTX > HTX (Fig. 10). This sequence resembles the previous one except for the position of HTX. At potassium channels, sensitivity, expressed by the half-decay time of the action-potential falling phase during repetitive stimulation (3.5 μM), the rank order was H_4-HTX > HTX > neo-H_2-HTX > iso-H_2-HTX ≈ H_8-HTX > iso-H_4-HTX > H_{12}-HTX > *N*-methyl-H_{12}-HTX. Despite these somewhat different sensitivities to structural modifications in the toxins, it seems significant that the effects at all three channels were accelerated by repetitive stimulation (see Figs. 5 and 9–11). Only the effects on epc τ were independent of stimulus frequency (see Table 2). The possibility that a common channel subunit or binding site, vulnerable to blockade by HTXs, subserves several types of ion channel is supported by the reports that glutamate responses[8] (26) are blocked by HTXs. In addition, iso-H_2-HTX noncompetitively inhibits binding of scopolamine to muscarinic receptors in neural cell lines (27). It is possible that the HTX binding site responsible for blockade of the various channels lies behind the gates that modulate current flow. However, it is noteworthy that an intrinsic structural protein of 43,000 mol wt which associates with but is not part of the AChR (17, 28) has also been reported to bind HTX with high affinity [$K_d = 7 \times 10^{-7}$ M, (29)]. This, taken with the hydrophobic nature of the toxins (except azaspiro-HTX, which is far weaker than the rest) as well as evidence discussed elsewhere (1), permits the speculation that the lipid-protein interface (the "annular lipids") is a possible common site at which the HTXs bind.

At the AChR two effects of HTXs were seen in epc experiments: a depression in both peak amplitude and a decrease in τ. These effects seemed independent of each other for the following reasons: (a) the time courses for onset were clearly distinguishable, with maximal depression of τ being attained much faster than maximal depression in the peak amplitude (Fig. 3); (b) peak amplitude, but not τ, in the presence of HTXs shows time and voltage dependence that generates hysteresis in peak amplitude versus voltage plots (13); and (c) repetitive stimulation progressively reduces peak amplitude (Fig. 5) but not τ (Table 2). It is not known whether this dichotomy in the actions of the toxins reflects two different binding sites or a single topographical site capable of two conformations, one of which alters τ and the other of which immobilizes the AChR in its closed form. Most studies of [^{3}H]H_{12}-HTX binding find only a single noninteracting population of binding sites in *Torpedo* electroplax membrane fragments with a dissociation constant (measured at equilibrium) of around 0.1–1.0 μM, depending on the conditions and preparations used (9, 11, 15–18). However, more recent studies have revealed that AChR activation by an agonist correlates with a faster rate of [^{3}H]H_{12}-HTX binding (12, 18). The site or conformation that binds [^{3}H]H_{12}-HTX when the AChR is activated with an agonist appears likely to be the one associated with progressive depression of epc amplitude during repetitive stimulation. The resting conformation or site which binds [^{3}H]H_{12}-HTX in the absence of agonist appears likely to be the one associated with alteration in τ.

If H_{12}-HTX were depressing τ by simply occluding the opened ion channels, one would expect the plot of τ^{-1} versus toxin concentration to be linear, at least until the decay of ACh concentration in the synaptic cleft becomes rate-limiting (at $\tau^{-1} > 1.7$ msec^{-1}). The reason is that, at the time of the epc peak, channels can close by the normal process (α below) or by combining with the toxin (D) to produce a nonconducting AChR*D.

$$A_2R \overset{\alpha}{\leftarrow} A_2R^* \underset{k_{-1}}{\overset{k_1}{\rightleftharpoons}} A_2R^*D \qquad (1)$$

Here, A is the agonist, R is the AChR, R^* is the activated

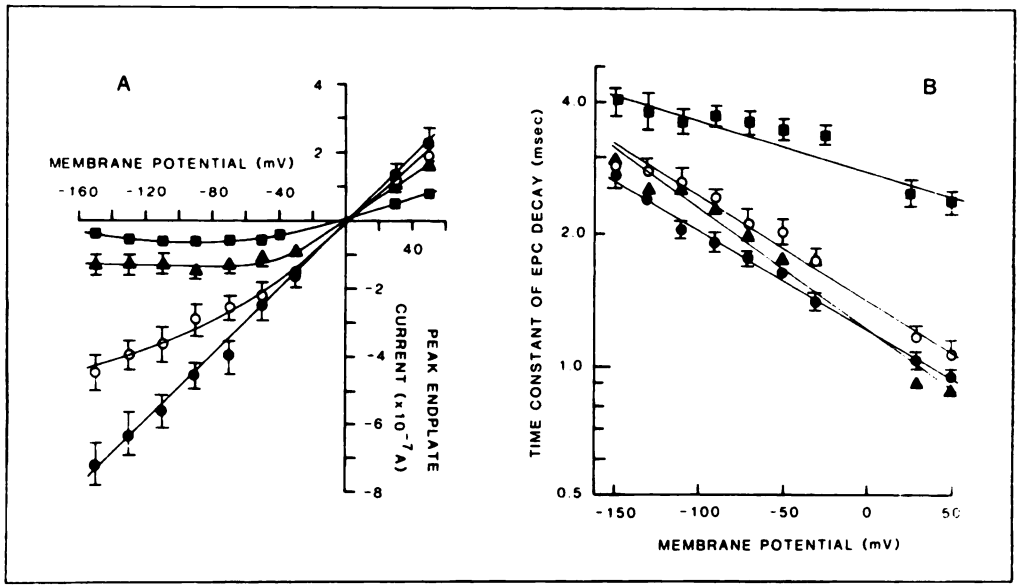

FIG. 8. *Epc peak amplitudes (A) and decay time constants (B) under control conditions (●) and in the presence of various concentrations of azaspiro-HTX*

Each symbol represents the mean ± standard error of at least six fibers from at least two muscles. The azaspiro-HTX concentrations shown are 100 (○), 400 (▲), and 600 (■) μM. The increase in τ at high azaspiro-HTX concentrations is complicated by the presence of ethanol used in the stock solution.

(open channel) AChR, D is H_{12}-HTX, and k_1 and k_{-1} are the rate constants for blocking and unblocking the channel, respectively. This sequential model has been used to describe the open channel blockade by a number of drugs (see ref. 1). When k_{-1} was small compared with $k_1[D]$, the epc decayed by a single exponential function of time, with a time constant $\tau^{-1} = \alpha + [D]k_1$. When H_{12}-HTX was present, only single exponential decays were observed, but the plot of τ^{-1} versus $[D]$ was not linear (Fig. 4B, *inset*). Therefore, we propose that a binding site exists which, when occupied by H_{12}-HTX, lowers the activation energy for channel closure. However, under

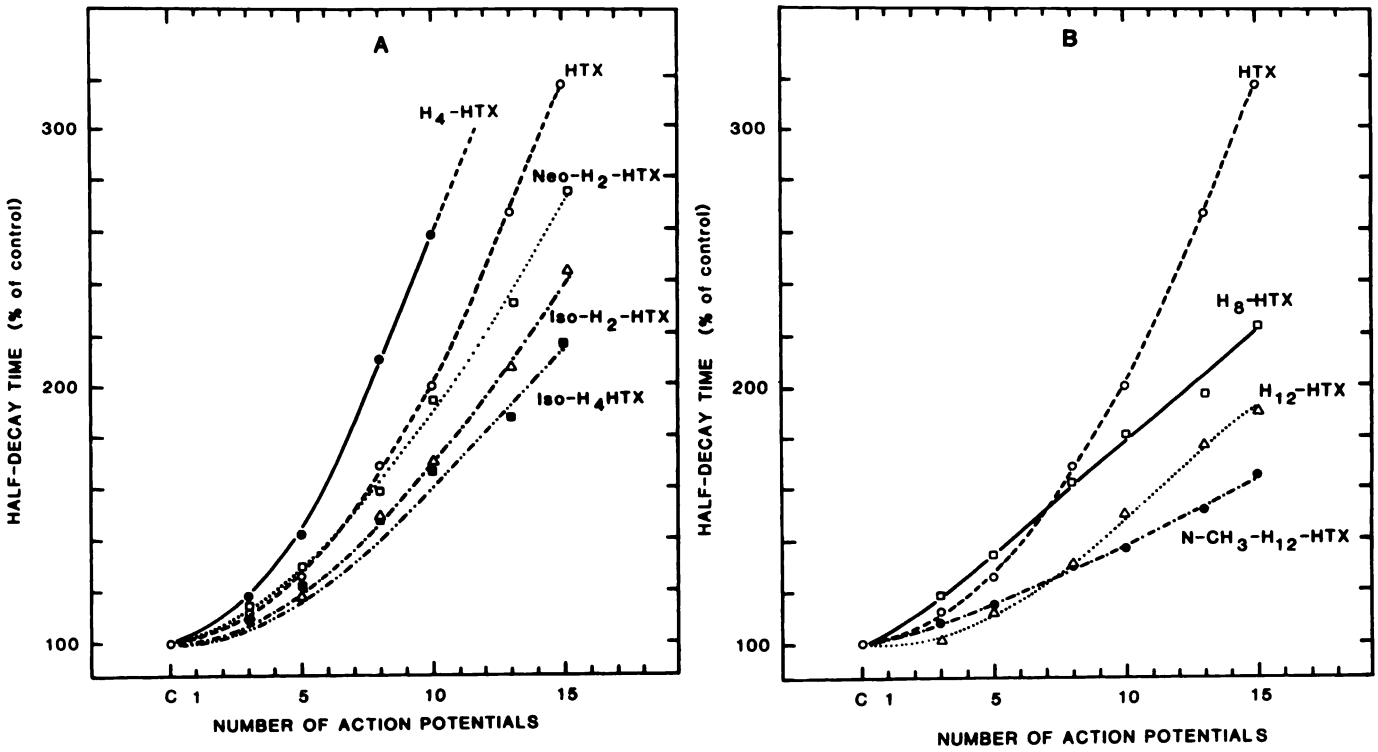

FIG. 9. *Half-decay times of muscle action potentials during repetitive stimulation (1 Hz) in the presence of various histrionicotoxins (3.5 μM) (A and B)*

Values are expressed as percentages of controls. Muscles were glycerol-shocked before beginning the experiment and treated with the toxins for 20 min prior to recording.

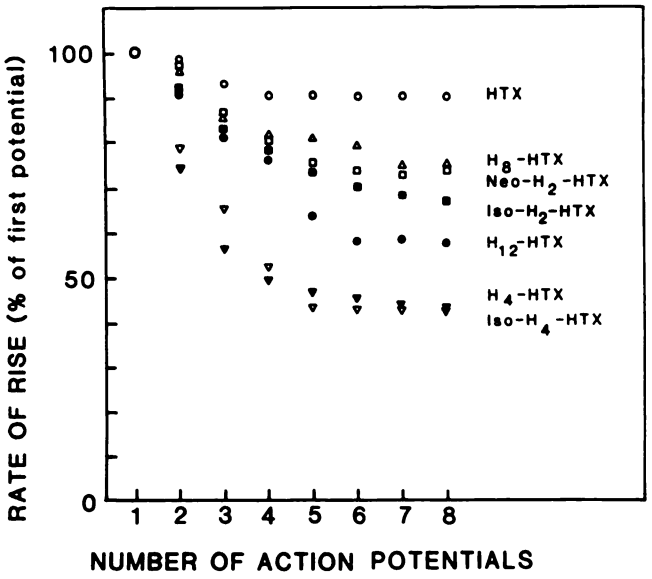

FIG. 10. *Maximal rates of rise in muscle action potentials during repetitive stimulation (1 Hz) in the presence of various histrionicotoxins (70 μM)*

Values are expressed as percentages of control. Muscles were glycerol-shocked before the experiment and treated with the toxins for 20 min prior to recording.

conditions of partial saturation one expects double exponential decays, since part of the population decays at a rate different from the rest. There are two possible reasons why this was not seen. One is that, since the decay time constants differed by no more than a factor of around 2, even at the most hyperpolarizing potentials (see Fig. 5B), such a small departure from single exponential decay could not be discerned. The second explanation is that all sites are in constant equilibrium, even during the millisecond time scale for epc decay. This latter model, used here and developed fully elsewhere,[9]

[9] L. A. Oliveira, A. T. Eldefrawi, M. E. Eldefrawi, and E. X. Albuquerque. Mechanism of action of naltrexone on the ionic channel of the nicotinic acetylcholine receptor. In preparation.

is represented as

$$\begin{array}{ccc} A_2R & \underset{\alpha}{\overset{\beta}{\rightleftharpoons}} & A_2R^* \\ D\downarrow\uparrow D & & D\downarrow\uparrow D \quad K \\ A_2RD & \underset{\alpha'}{\overset{\beta'}{\rightleftharpoons}} & A_2R^*D \end{array} \qquad (2)$$

Note that in this scheme A_2R^*D does conduct ionic current. The primed-rate constants result when the AChR is occupied by H_{12}-HTX. The rate constant for channel closure is simply given by

$$\tau^{-1} = \frac{\alpha + \alpha' K[D]}{1 + K[D]} \qquad (3)$$

Equation 3 may be derived simply by denoting the sum of the open channels as $A = [AR^*] + [AR^*D]$ and by expressing $[AR^*D]$ in terms of $[AR^*]$, as dictated by the assumed equilibrium condition (i.e., $[AR^*D] = [AR^*][D]K$). Solution of the differential equation

$$\frac{-dA}{dt} = A\frac{\alpha + \alpha' K[D]}{1 + K[D]}$$

yields Eq. 3. The formal comparison to a simple, saturating, ligand binding curve, as mentioned under Results (see Fig. 4B, *inset*), is now evident. At each membrane potential the parameters α, α', and K were evaluated by nonlinear regression analysis (22) of all epc decays (around 80) available at all H_{12}-HTX concentrations. The parameter estimates are plotted in Fig. 13. The parameter values in the *lower line* in 13A (▲) are estimates of α, and those of the *upper line* in 13A (●) are estimates of α', the rate constant for channel closure when all of the toxin sites are occupied by H_{12}-HTX. At zero membrane potential, α' is greater than α, implying that the activation energy for channel closure is decreased. In addition, the voltage sensitivity for α', expressed as the slope of the semilogarithm plot of τ versus membrane potential (Fig. 13A), is also decreased, suggesting that the change

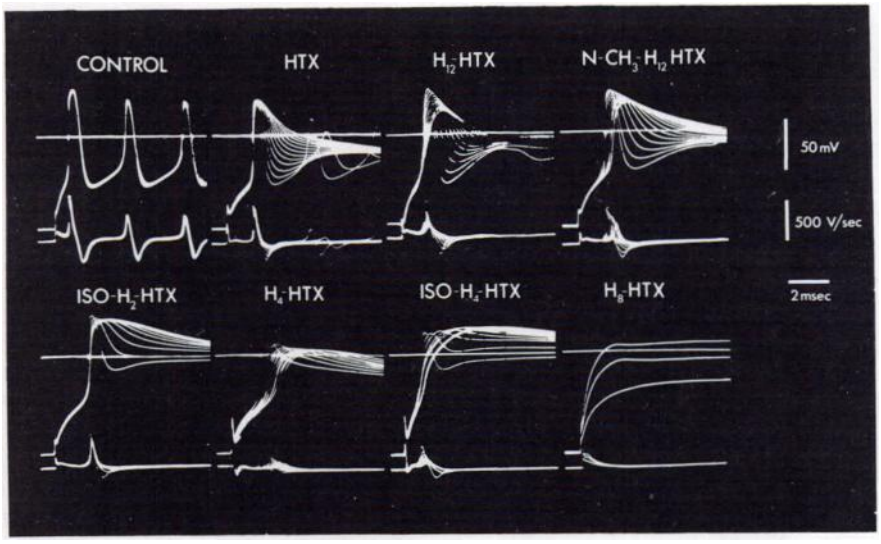

FIG. 11. *Muscle action potentials during repetitive stimulation (1 Hz) in the presence of various histrionicotoxins (70 μM)*
Muscles were glycerol-shocked before beginning the experiment and treated with the toxins for 20 min prior to recording.

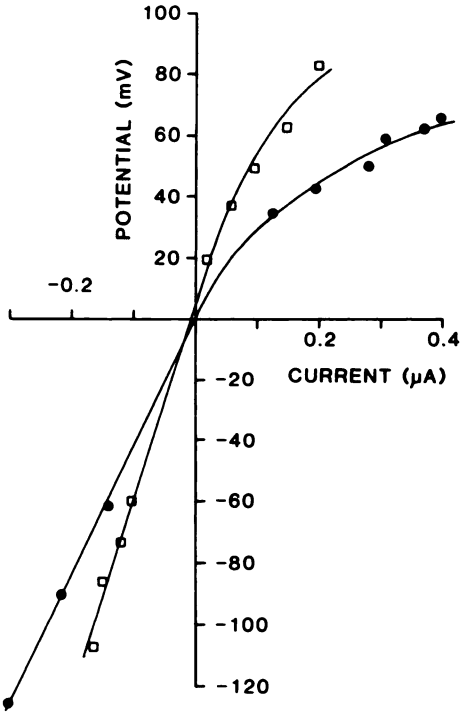

FIG. 12. *Delayed rectification under control conditions (●) and in the presence of 70 μM neo-H_2-HTX (□)*

The muscle was bathed in tetrodotoxin (3 μM)-Ringer's throughout and treated with neo-H_2-HTX for 30 min prior to recording. The membrane current was measured 30 msec after the voltage jump.

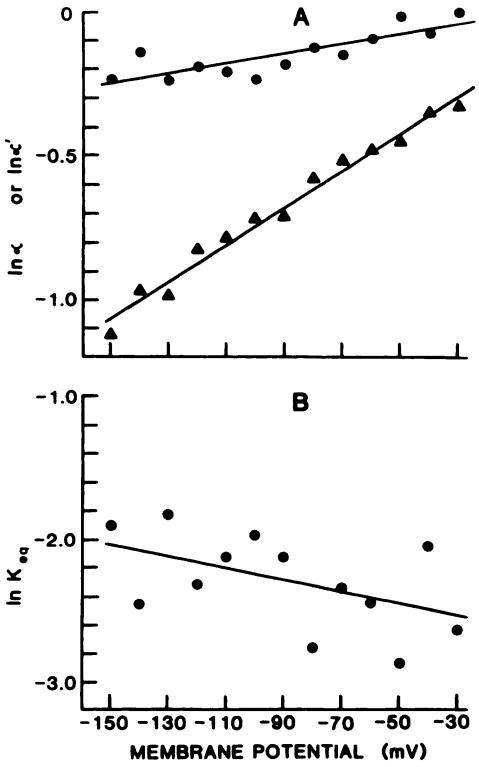

FIG. 13. *Estimates of nonlinear regression parameter values for the rate constants of channel closure (A) and the equilibrium constants for H_{12}-HTX binding (B)*

Values are referenced per millisecond in A and per micromolar in B. In A, estimates of α (△) and α' (●) are shown. At each membrane potential, the three parameter estimates shown here (α, α', and K) were obtained from nonlinear regression analysis of about 80 epc decay τs and based on Eq. 3. These epcs were recorded under control conditions and in the presence of 2, 5, 10, 30, and 40 μM H_{12}-HTX (see Fig. 4). The lines shown resulted from linear regression of the logarithm of the parameter estimates on membrane potential.

in AChR dipole moment believed to accompany the closure (30) is decreased. The affinity constant, K (Fig. 13B), appears to be slightly voltage-sensitive (the slope of the linear regression line is significantly different from zero only at $p < 0.10$), and from the slope of the linear regression one may calculate the depth of H_{12}-HTX penetration into the transmembrane electric field at its binding site to be 10% ± 5 (SD). Alternatively, the electric field may slightly distort the H_{12}-HTX binding site. All of the semilog plots in Fig. 13 seemed to be linear functions of membrane potential and had similar variances. From linear regression analysis, therefore, one can fit each of the parameters to the form $\ln P = \ln P_0 + AV$, where P_0 is the value of the parameter when membrane potential is 0 mV. These six parameters, shown in Table 3, were used to predict the τ values plotted as *solid curves* in Fig. 4B. All of the experimental τ values (except those at 30 μM H_{12}-HTX), from control to 40 μM, and membrane potentials covering a 120-mV range were predicted satisfactorily by this model.

TABLE 3

Parameter estimates for rate constants α and α' and affinity constant K

The parameters are expressed in the form $\ln P_v = \ln P_0 + AV$, where V is membrane potential in millivolts. Means ± standard deviation of the parameter estimates are shown.

Parameter	$\ln P_0$	A
		mV^{-1}
α, $msec^{-1}$	−0.098 ± 0.027	0.0064 ± 0.00028
α', $msec^{-1}$	0.014 ± 0.034	0.0018 ± 0.00035
K, μM^{-1}	−2.64 ± 0.20	−0.0040 ± 0.0020

The HTX data also seemed to fit this model. The curve shown in Fig. 6B, *inset*, was based on Eq. 3 and the parameters $(hdt)^{-1} = 0.56$ $msec^{-1}$, $(hdt')^{-1} = 1.22$ $msec^{-1}$, and $K_{aff} = 0.080$ μ^{-1}. By comparison, the 95% confidence interval for the H_{12}-HTX K_{aff} is 0.12–0.087 μM^{-1}, which cannot be confidently distinguished from K_{aff} for HTX. In general, the HTX data were too scattered to permit as detailed an analysis as was done with H_{12}-HTX.

In conclusion, all of the HTXs, except perhaps azaspiro-HTX, displayed a family resemblance to one another in their qualitative actions at the AChR and voltage-sensitive sodium and potassium channels. However, no rank order of potency applied uniformly to these three types of channel. Evidence from epcs suggested that two independent sites or conformations are targets for these toxins at the AChR, one of which alters activation kinetics and the other of which prevents the channel from opening. Open channel occlusion is eliminated as a mechanism for blockade.

ACKNOWLEDGMENT

We are indebted to Ms. Mabel Alice Zelle for expert computer analysis and general technical assistance.

REFERENCES

1. Spivak, C. E. and E. X. Albuquerque. The dynamic properties of the nicotinic receptor ionic channel complex: activation and blockade, in *Progress in Cholinergic Biology: Models of Cholinergic Synapses* (I. Hamin and A. Goldberg, eds.). Raven Press, New York, in press (1982).
2. Daly, J. W., I. Karle, C. W. Myers, T. Tokuyama, J. A. Waters, and B. Witkop. Histrionicotoxins: roentgen-ray analysis of the novel allenic and acetylenic spiroalkaloids isolated from a Colombian frog, *Dendrobates histrionicus*. *Proc. Natl. Acad. Sci. U. S. A.* **68**:1870–1875 (1971).
3. Tokuyama, T., K. Uenoyama, G. Brown, J. W. Daly, and B. Witkop. Allenic and acetylenic spiropiperidine alkaloids from the neotropical frog, *Dentrobates histrionicus*. *Helv. Chim. Acta* **57**:2597–2604 (1974).
4. Albuquerque, E. X., E. A. Barnard, T. H. Chiu, A. J. Lapa, J. O. Dolly, S.-E. Jansson, J. Daly, and B. Witkop. Acetylcholine receptor and ion conductance modulator sites at the murine neuromuscular junction: evidence from specific toxin reactions. *Proc. Natl. Acad. Sci. U. S. A.* **70**:949–953 (1973).
5. Albuquerque, E. X., K. Kuba, A. J. Lapa, J. W. Daly, and B. Witkop. Acetylcholine receptor and ionic conductance modulator of innervated and denervated muscle membranes: effect of histrionicotoxins, in *Exploratory Concepts in Muscular Dystrophy* (A. T. Milhorat, ed.), Vol. II. Excerpta Medica, Amsterdam, 585–600 (1973).
6. Lapa, A. J., E. X. Albuquerque, J. M. Sarvey, J. Daly, and B. Witkop. Effects of histrionicotoxin on the chemosensitive and electrical properties of skeletal muscle. *Exp. Neurol.* **47**:558–580 (1975).
7. Albuquerque, E. X., K. Kuba, and J. Daly. Effect of histrionicotoxin on the ionic conductance modulator of the cholinergic receptor: a quantitative analysis of the end-plate current. *J. Pharmacol. Exp. Ther.* **189**:513–524 (1974).
8. Albuquerque, E. X., and A. C. Oliveira. Physiological studies on the ionic channel of nicotinic neuromuscular synapses. *Adv. Cytopharmacol.* **3**:197–211 (1979).
9. Elliot, J., and M. A. Raftery. Interactions of perhydrohistrionicotoxin with postsynaptic membranes. *Biochem. Biophys. Res. Commun.* **77**:1347–1353 (1977).
10. Eldefrawi, M. E., and A. T. Eldefrawi. Biochemical studies on the ionic channel of *Torpedo* acetylcholine receptor. *Adv. Cytopharmacol.* **3**:213–223 (1979).
11. Elliott, J., and M. A. Raftery. Binding of perhydrohistrionicotoxin to intact and detergent-solubilized membranes enriched in nicotinic acetylcholine receptor. *Biochemistry* **18**:1868–1874 (1979).
12. Eldefrawi, M. E., R. S. Aronstam, N. M. Bakry, A. T. Eldefrawi, and E. X. Albuquerque. Activation, inactivation, and desensitization of acetylcholine receptor channel complex detected by binding of perhydrohistrionicotoxin. *Proc. Natl. Acad. Sci. U.S.A.* **77**:2309–2313 (1980).
13. Masukawa, L. M., and E. X. Albuquerque. Voltage- and time-dependent action of histrionicotoxin on the endplate current of the frog muscle. *J. Gen. Physiol.* **72**:351–367 (1978).
14. Anwyl, R., and T. Narahashi. Inhibition of the acetylcholine receptor by histrionicotoxin. *Br. J. Pharmacol.* **68**:611–615 (1980).
15. Eldefrawi, A. T., M. E. Eldefrawi, E. X. Albuquerque, A. C. Oliveira, N. Mansour, M. Adler, J. W. Daly, G. B. Brown, W. Burgermeister, and B. Witkop. Perhydrohistrionicotoxin: a potential ligand for the ion conductance modulator of the acetylcholine receptor. *Proc. Natl. Acad. Sci. U.S.A.* **74**:2172–2176 (1977).
16. Eldefrawi, M. E., A. T. Eldefrawi, N. A. Mansour, J. W. Daly, B. Witkop, and E. X. Albuquerque. Acetylcholine receptor and ionic channel of *Torpedo* electroplax: binding of perhydrohistrionicotoxin to membrane and solubilized preparations. *Biochemistry* **17**:5474–5484 (1978).
17. Elliott, J., S. M. J. Dunn, S. G. Blanchard, and M. A. Raftery. Specific binding of perhydrohistrionicotoxin to *Torpedo* acetylcholine receptor. *Proc. Natl. Acad. Sci. U.S.A.* **76**:2576–2579 (1979).
18. Aronstam, R. S., A. T. Eldefrawi, I. N. Pessah, J. W. Daly, E. X. Albuquerque, and M. E. Eldefrawi. Regulation of [^{3}H]perhydrohistrionicotoxin binding to *Torpedo ocellata* electroplax by effectors of the acetylcholine receptor. *J. Biol. Chem.* **256**:2843–2850 (1981).
19. Gage, P. W., and R. S. Eisenberg. Action potentials without contraction in frog skeletal muscle fibers with disrupted transverse tubules. *Science* (*Wash. D.C.*) **158**:1702–1703 (1967).
20. Kuba, K., E. X. Albuquerque, J. Daly, and E. A. Barnard. A study of the irreversible cholinesterase inhibitor, diisopropylfluorophosphate, on time course of end-plate currents in frog sartorius muscle. *J. Pharmacol. Exp. Ther.* **189**:499–512 (1974).
21. Gössinger, E., R. Imhof, and H. Wehrli. Modell zersuche in der Histrionicotoxinreihe: Synthese des (±)-Cis-1-azaspiro[5.5]undecan-8-ols. *Helv. Chim. Acta* **58**:96–103 (1975).
22. Dixon, W. J., and M. B. Brown (eds.). *BMDP-79 Biomedical Computer Programs P Series*. University of California Press, Los Angeles, 464–483 (1979).
23. Katz, B., and S. Thesleff. A study of the 'desensitization' produced by acetylcholine at the motor end-plate. *J. Physiol.* (*Lond.*) **138**:63–80 (1957).
24. Magleby, K. L., B. S. Pallotta, and D. A. Terrar. The effect of (+)-tubocurarine on neuromuscular transmission during repetitive stimulation in the rat, mouse, and frog. *J. Physiol.* (*Lond.*) **312**:97–113 (1981).
25. Gage, P. W., R. N. McBurney, and G. T. Schneider. Effects of some aliphatic alcohols on the conductance change caused by a quantum of acetylcholine at the toad end-plate. *J. Physiol.* (*Lond.*) **244**:409–429 (1975).
26. Glavinović, M., J. L. Henry, G. Kato, K. Krnjević, and E. Puil. Histrionicotoxin: effects on some central and peripheral excitable cells. *Can. J. Physiol. Pharmacol* **52**:1220–1226 (1974).
27. Burgermeister, W., W. L. Klein, M. Nirenberg, and B. Witkop. Comparataive binding studies with cholinergic ligands and histrionicotoxin at muscarinic receptors of neural cell lines. *Mol. Pharmacol.* **14**:751–767 (1978).
28. Neubig, R. R., E. K. Krodel, N. D. Boyd, and J. B. Cohen. Acetylcholine and local anesthetic binding to *Torpedo* nicotinic postsynaptic membranes after removal of nonreceptor peptides. *Proc. Natl. Acad. Sci. U.S.A.* **76**:690–694 (1979).
29. Sobel, A., T. Heidmann, J. Hofler, and J.-P. Changeux. Distinct protein components from *Torpedo marmorata* membranes carry the acetylcholine receptor site and the binding site for local anesthetics and histrionicotoxin. *Proc. Natl. Acad. Sci. U.S.A.* **75**:510–514 (1978).
30. Magleby, K. L., and C. F. Stevens. A quantitative description of end-plate currents. *J. Physiol.* (*Lond.*) **223**:173–197 (1972).

Send reprint requests to: Dr. E. X. Albuquerque, Department of Pharmacology and Experimental Therapeutics, University of Maryland School of Medicine, Baltimore, Md. 21201.